Chapter 12
A Trefftz Method for the Time-Harmonic Eddy Current Equation

Raffael Casagrande, Christoph Winkelmann, Ralf Hiptmair, and Jörg Ostrowski

Abstract We present a discontinuous finite element method to resolve the skin effect in conductors on coarse meshes. The idea is to take into account the exponential decay in the finite element trial space, which enables to resolve the skin layer independent of the size of the mesh cells. The discontinuous, Trefftz-type basis functions are coupled across the element boundaries by the interior penalty-/Nitsche's method and numerical experiments affirm the effectiveness of the method for thin boundary layers.

12.1 Introduction

We consider the vector potential formulation of the eddy current problem in the frequency domain with temporal gauge ($\varphi = 0$),

$$\mathbf{curl}\left(\mu^{-1}\mathbf{curl}\mathbf{A}\right) + i\omega\sigma\mathbf{A} = \mathbf{j}^i. \tag{12.1}$$

Here

- $\mathbf{A}(\mathbf{x})$ is a vector potential,
- $\mathbf{B} = \nabla \times \mathbf{A}$ is the magnetic flux density,
- $\mathbf{j}^i(\mathbf{x})$ is the impressed, solenoidal electric current,
- $\omega > 0$ is the angular frequency, and
- $\sigma(\mathbf{x})$ is the electric conductivity (which can be zero in parts of the domain and is assumed to be piecewise constant).

R. Casagrande (✉) · C. Winkelmann · R. Hiptmair
Seminar for Applied Mathematics, ETH Zürich, Zürich, Switzerland
e-mail: raffael.casagrande@sam.math.ethz.ch; christoph.winkelmann@sam.math.ethz.ch; hiptmair@sam.math.ethz.ch

J. Ostrowski
ABB Switzerland Ltd., Corporate Research, Baden, Switzerland
e-mail: joerg.ostrowski@ch.abb.com

© Springer International Publishing AG, part of Springer Nature 2018

U. Langer et al. (eds.), *Scientific Computing in Electrical Engineering*, Mathematics in Industry 28, https://doi.org/10.1007/978-3-319-75538-0_12

It is well known that the solution of (12.1) exhibits singularities in edges (and corners) of conductors [4], as well as exponential boundary layers along the surface of conductors (*skin effect*). I.e. the induced current $i\omega\sigma\mathbf{A}$ is concentrated at the surface of conductors and decays rapidly towards the interior. The thickness of the boundary layer is characterized by the skin-depth δ.

Induction has many applications in industry. An example is inductive hardening [8], where the workpiece is heated quickly at the surface, and is then rapidly cooled down before the heat is distributed into the interior by heat conduction. In this case the skin effect plays a fundamental technical role and resolving the skin layer is essential.

For the classical low order Finite Element Method (FEM) this means that the boundary layers must be resolved by the underlying mesh. This can be achieved by adapting the mesh manually or by refining an existing mesh towards the boundary layers, which can be automated (h-refinement). However, in industrial applications the skin depth δ can be orders of magnitude smaller than the diameter of the conductor so that the mesh must be refined multiple times towards the boundary layer(s). This leads to a vast increase in the number of degrees of freedom (DOF) which may render the solution of the linear system prohibitively expensive.

Alternatively one can refine the mesh just once to create a mesh layer of thickness $O(k\delta)$ where k is the polynomial degree of the test functions [9, 10]. However creating such a 3D mesh for industrial applications can be hard, especially if tetrahedral elements are used.

A partial remedy for this problem are Impedance Boundary Conditions (IBC) [8]: The conductor is replaced by Robin-type boundary conditions and the electromagnetic fields are only calculated at the surface of the conductor. Since the IBC approximation assumes that the conductor surface is flat, the solution deteriorates as the radius of curvature of the conductor surface becomes comparable to the skin-depth δ. In particular the IBC solution deviates strongly from the physically correct fields at edges and corners of the conductor.

In this work we propose to resolve the boundary layers directly on coarse meshes (we assume the meshsize $h \gg \delta$) by enriching the approximation space with suitable functions. More precisely, our approximation space will contain two types of (discontinuous) basis functions:

- Edge elements R_k [7], and
- Exponential boundary layer functions modulated/multiplied with polynomials.

We deal with the discontinuous nature of the basis functions in the framework of Discontinuous Galerkin (DG) methods and discretize (12.1) by the Non-Symmetric Weighted Interior Penalty (NWIP) method [3].

12.2 Non-symmetric Weighted Interior Penalty Framework

We consider the time-harmonic eddy current equation (12.1) on a bounded, open, polyhedral domain $\Omega \subset \mathbb{R}^3$ with Lipschitz boundary. Furthermore we denote by $\Omega_0 \subset \Omega$ the open subdomain where $\sigma = 0$ and define $\Omega_\sigma = \Omega \setminus \overline{\Omega_0}$.

Perturbed Problem It is well-known that the time-harmonic eddy current equation (12.1) does not uniquely determine the vector potential $\mathbf{A}$ in Ω_0, i.e. (12.1) is an ungauged formulation. In this work we restore the uniqueness of $\mathbf{A}$ by considering the *perturbed* time-harmonic eddy current problem [1],

$$\mathbf{curl}\left(\mu^{-1}\mathbf{curl}\mathbf{A}^\alpha\right) + \kappa^\alpha \mathbf{A}^\alpha = \mathbf{j}^i, \qquad \text{in } L^2(\Omega)^3 \tag{12.2a}$$

$$\mathbf{n} \times \mathbf{A}^\alpha = 0 \qquad \text{on } \partial\Omega. \tag{12.2b}$$

Here the boundary condition (12.2b) implies $\mathbf{n} \cdot \mathbf{curl}\mathbf{A} = \mathbf{n} \cdot \mathbf{B} = 0$ which reflects the decay of the magnetic field far away from the source $\mathbf{j}^i$. Moreover,

$$\kappa^\alpha(\mathbf{x}) := \begin{cases} i\omega\sigma(\mathbf{x}) & \text{for } x \in \Omega_\sigma, \\ \alpha & \text{for } x \in \Omega_0, \end{cases}$$

with $\alpha > 0$ being the regularization parameter. One expects that for $\alpha \to 0$ also $\mathbf{A}^\alpha \to \mathbf{A}$, or more precisely [1, Lemma 33],

Lemma 12.1 *Under the above assumptions we have,* $\|\mathbf{A} - \mathbf{A}^\alpha\|_{\mathbf{H(curl};\Omega)} \leq C\alpha \|\mathbf{A}\|_{L^2(\Omega)^3}$*, where* C *is independent of* α *but depends on* μ*,* σ*,* ω *and the domain* Ω*.*

Broken Sobolev Spaces We assume that there exists a partition $P_\Omega = \{\Omega_i\}_i$ such that each Ω_i is a polyhedron and such that the permeability $0 < \mu < \infty$ and the coefficient function $0 < \kappa^\alpha < \infty$ are constant on each Ω_i. We will assume that the solution $\mathbf{A}^\alpha$ lies in the broken Sobolev space

$$V^*(P_\Omega) := \left\{ \mathbf{A} \in L^2(\Omega)^3 \,\middle|\, \mathbf{A}|_K \in H^1(K)^3,\ \mathbf{curl}\mathbf{A}|_K \in H^1(K)^3\ \forall K \in P_\Omega \right\}.$$

Here $H^1(K) := \{f \in L^2(K) |\ \mathbf{grad}\, f \in L^2(K)^3\}$ denotes the usual Sobolev space.

Meshes, Jumps, Averages Let $\mathscr{T}_h$ denote a hybrid (tetrahedras, pyramids, prisms, hexahedras), affine, conforming mesh on Ω that is *compatible* with the partition P_Ω, that is every mesh element $T \in \mathscr{T}_h$ lies in exactly one $\Omega_i \in P_\Omega$. Thus κ^α, μ are constant on every mesh cell $T \in \mathscr{T}_h$ and we have $V^*(P_\Omega) \subset V^*(\mathscr{T}_h)$. Furthermore we let $\mathscr{F}_h^i$ denote the set of inner intersections of $\mathscr{T}_h$ and define the tangential jump and *weighted* average of a vector valued function $\mathbf{A} \in V^*(\mathscr{T}_h)$ on an inner face $F \in \mathscr{F}_h^i$, $F = \partial T_i \cap \partial T_j$, as follows:

$$[\![\mathbf{A}_h]\!]_T = \mathbf{n}_F \times \left(\mathbf{A}_h|_{T_i} - \mathbf{A}_h|_{T_j}\right), \qquad \text{(jump)}$$

$$\{\!\{\mathbf{A}_h\}\!\}_w = w_1\, \mathbf{A}_h|_{T_i} + w_2\, \mathbf{A}_h|_{T_j}, \qquad \text{(average)}$$

Here $\mathbf{n}_F$ always points from T_i to T_j and $w_i \in [0, 1]$ are such that $w_1 + w_2 = 1$.

NWIP-Formulation We discretize the perturbed eddy current problem (12.2) using a *finite dimensional* subspace $V_h \subset V_h^* := \{\mathbf{A} \in V^*(\mathscr{T}_h) | \ \mathbf{n} \times \mathbf{A} = 0 \text{ on } \partial\Omega\}$. Multiplying (12.2) with a discontinuous test function $\mathbf{A}'_h \in V_h$ and integrating by parts on each element, one arrives at [3]: Find $\mathbf{A}^\alpha_h \in V_h$ such that for all $\mathbf{A}'_h \in V_h$:

$$a_h^{\mathrm{NWIP}}(\mathbf{A}^\alpha_h, \mathbf{A}'_h) + \int_\Omega \kappa^\alpha \mathbf{A}^\alpha_h \cdot \overline{\mathbf{A}'_h} = \int_\Omega \mathbf{j}^i \cdot \overline{\mathbf{A}'_h}, \tag{12.3}$$

with sesquilinear form

$$\begin{aligned} a_h^{\mathrm{NWIP}}(\mathbf{A}^\alpha_h, \mathbf{A}'_h) := &\int_\Omega \mu^{-1} \mathbf{curl}\mathbf{A}^\alpha_h \cdot \mathbf{curl}\overline{\mathbf{A}'_h} - \sum_{F \in \mathscr{F}_h^i} \int_F \left\{\!\!\left\{ \mu^{-1} \mathbf{curl}\mathbf{A}^\alpha_h \right\}\!\!\right\}_w \cdot \overline{[\![\mathbf{A}'_h]\!]_T} \\ &+ \sum_{F \in \mathscr{F}_h^i} \int_F \overline{\left\{\!\!\left\{ \mu^{-1} \mathbf{curl}\mathbf{A}'_h \right\}\!\!\right\}_w} \cdot [\![\mathbf{A}^\alpha_h]\!]_T + \sum_{F \in \mathscr{F}_h^i} \frac{\eta \gamma_{\mu,F}}{h_F} \int_F [\![\mathbf{A}^\alpha_h]\!]_T \cdot \overline{[\![\mathbf{A}'_h]\!]_T}. \end{aligned}$$

Here h_F is the diameter of face F and $\eta > 0$ is the penalty parameter. The weights for an inner face $F = \partial T_1 \cap \partial T_2$ are chosen as

$$\gamma_{\mu,\mathrm{F}} := \frac{2}{\mu_1 + \mu_2}, \qquad w_1 := \frac{\mu_1}{\mu_1 + \mu_2}, \qquad w_2 := \frac{\mu_2}{\mu_1 + \mu_2}.$$

We have the following best approximation result, cf. [3, Theorem 3.3.13]:

Theorem 12.1 *Let $\mathbf{A}^\alpha \in V^*(P_\Omega)$ be the solution of the perturbed problem (12.2) and let $\mathbf{A}^\alpha_h \in V_h$ solve the NWIP formulation (12.3). Then there exist constants $C > 0$, $C_\eta > 0$, both independent of h, μ, κ such that for $\eta > C_\eta$*

$$\left\| \mathbf{A}^\alpha - \mathbf{A}^\alpha_h \right\|_{IP} < C \inf_{\mathbf{v}_h \in V_h} \| \mathbf{A} - \mathbf{v}_h \|_{IP,*}, \tag{12.4}$$

and the discrete problem (12.3) is well-posed. The constants C_η, C depend on the choice of the subspace $V_h \subset V_h^*$ and C_η depends on C.

The associated (semi-) norms are defined as:

$$\|\mathbf{A}\|_{\mathrm{IP}}^2 := \left\| \mu^{-1/2} \mathbf{curl}\mathbf{A} \right\|_{L^2(\Omega)^3}^2 + \left\| \sqrt{|\kappa^\alpha|}\mathbf{A} \right\|_{L^2(\Omega)^3}^2 + \sum_{F \in \mathscr{F}_h^i} \frac{\gamma_{\mu,F}}{h_F} \left\| [\![\mathbf{A}]\!]_T \right\|_{L^2(F)^3}^2,$$

$$\|\mathbf{A}\|_{\mathrm{IP},*}^2 := \|\mathbf{A}\|_{\mathrm{IP}}^2 + \sum_{T \in \mathscr{T}_h} h_T \left\| \mu^{-1/2} \mathbf{curl}\mathbf{A} \right\|_{L^2(T)^3}^2.$$

12.3 Enriched Approximation Space

Trefftz Functions Let $\mathbf{n}$ be a unit vector and consider problem (12.1) on the whole space $\mathbb{R}^3$ such that σ is zero in the half-space $\Omega_0 = \{\mathbf{x} \in \mathbb{R}^3 |\ \mathbf{x} \cdot \mathbf{n} > 0\}$ and equal to a positive constant σ in the other half-space $\Omega_\sigma = \mathbb{R}^3 \setminus \overline{\Omega_0}$. Furthermore, assume that there is an external excitation by a magnetic field $\mathbf{H}_0$ which is constant along the surface $F := \{\mathbf{x} \in \mathbb{R}^3 |\ \mathbf{x} \cdot \mathbf{n} = 0\}$ and that $\mu \equiv const$, $\mathbf{j}^i = 0$ in Ω_σ. Simple manipulations (cf. [5]) show that inside the conductor Ω_σ ($\mathbf{x} \cdot \mathbf{n} < 0$) we can write the solution $\mathbf{A}$ of (12.1) explicitly as

$$\mathbf{A}(\mathbf{x}) = \mathbf{A}_{F,\boldsymbol{\tau}}(\mathbf{x}) := |\mathbf{H}_0|\, \delta/(1+i)\ \boldsymbol{\tau}\ \exp\left((1+i)(\mathbf{x}-\mathbf{x}_0)\cdot\mathbf{n}/\delta\right), \tag{12.5}$$

where $\mathbf{x}_0 \in F$, $\boldsymbol{\tau} \in \mathbb{R}^3$ is a vector tangential to F, and $\delta = \sqrt{\frac{2}{\mu\sigma\omega}}$ is the skin-depth.

Modulated Trefftz Functions Let $\mathbb{P}_k(T)$ denote the space of polynomials of total degree $\leq k$ on mesh element $T \in \mathscr{T}_h$. For each element $T \in \mathscr{T}_h$, $T \subset \Omega_\sigma$ we define the space

$$\mathscr{A}_k(T) := \left\{ p\mathbf{A}_{F,\boldsymbol{\tau}} |\ p \in \mathbb{P}_k(T),\ F \in \mathscr{F}_h^i,\ F \subset \partial T \cap \partial\Omega_0,\ \boldsymbol{\tau} \text{ tangential of } F \right\}.$$

Note that the dimension of the space $\mathscr{A}_k(T)$ is $2n\dim(\mathbb{P}_k(T))$, where n is the number of faces of T that are at the conductor surface, since for every flat surface there are only two linearly independent tangentials $\boldsymbol{\tau}$. We define $\mathscr{T}_h^{\mathscr{A}} := \{T \in \mathscr{T}_h |\ \dim(\mathscr{A}_1(T)) > 0, \sigma(T) > 0\}$ to be the set of elements with at least one adjacent boundary layer and we let $\Omega_{\mathscr{A}} \subset \Omega$ be the union of all elements in $\mathscr{T}_h^{\mathscr{A}}$. We then define the *broken, modulated Trefftz approximation space* by

$$\mathscr{A}_k(\mathscr{T}_h) := \left\{ \mathbf{A} \in L^2(\Omega_{\mathscr{A}})^3 |\ \ \mathbf{A}|_T \in \mathscr{A}_k(T)\ \forall T \in \mathscr{T}_h^{\mathscr{A}} \right\}.$$

Broken Edge Element Space Our idea is to use a conforming edge element space wherever possible and to "break" this space only around elements containing the modulated Trefftz functions:

$$R_{k,\mathscr{A}}(\mathscr{T}_h) := \left\{ \mathbf{A} \in L^2(\Omega)^3 \,\middle|\, \mathbf{A}|_T \in R_k(T)\,\forall T \in \mathscr{T}_h,\ \mathbf{n}\times\mathbf{A} = 0 \text{ on } \partial\Omega, \right.$$
$$\left. \text{and}\quad \mathbf{A}|_{\Omega\setminus\overline{\Omega_{\mathscr{A}}}} \in \mathbf{H}(\mathbf{curl};\, \Omega \setminus \overline{\Omega_{\mathscr{A}}}) \right\}.$$

Here $R_k(T)$ is the space of k-th order edge elements of the first kind on mesh element $T \in \mathscr{T}_h$, cf. [2, 7] and $\mathbf{H}(\mathbf{curl};\, \Omega) := \{\mathbf{A} \in L^2(\Omega)^3 |\ \mathbf{curl}\mathbf{A} \in L^2(\Omega)^3\}$. We define the enriched approximation space V_h on mesh $\mathscr{T}_h$ as

$$V_h := R_{k,\mathscr{A}}(\mathscr{T}_h) \oplus \mathscr{A}_k(\mathscr{T}_h).$$

Note that this space is tangentially continuous across a face $F \in \mathscr{F}_h^i$ if and only if both the adjacent elements do *not* belong to $\mathscr{T}_h^{\mathscr{A}}$. I.e. the DG-terms on these faces drop out of the NWIP formulation (12.3) and the method resembles "locally" the standard finite element method. Moreover we note that V_h is a superset of the space of conforming edge elements, $R_{k,h} \coloneqq \{\mathbf{A} \in \mathbf{H}(\mathbf{curl}; \Omega) |\ \mathbf{A}|_T \in R_k(T)\ \forall T \in \mathscr{T}_h\}$. In light of the best approximation result (12.4) we can thus expect that the space V_h has equal or better approximation properties than the space $R_{k,h}$.

12.4 Numerical Example

We pose problem (12.2) on a cylindrical shaped domain Ω with two conductors Ω_σ: The "plate" Ω_{plate} (green) is the cuboid $(-0.7, -0.5) \times (-1, 1)^2$ whereas the "bar" (gray) has dimensions $(0.5, 1.5) \times (-2.5, 2.5) \times (-0.5, 0.5)$. We mesh Ω with the coarse, hybrid mesh $\mathscr{T}_h$ shown in Fig. 12.1 that has only one layer of elements across the plate. This reflects the constraints encountered with more complex geometries where it is prohibitively expensive to resolve the boundary layers with a fine mesh.

The system is excited by a homogeneous generator current, $\mathbf{j}^i = (0, 2000, 0)$ in Ω_{bar}, which induces an electric current in the plate. We will vary σ_{plate} to simulate boundary layers of arbitrary thickness in the plate and keep all other (material) parameters constant: $\mu \equiv 4\pi \cdot 10^{-7}$ globally, $\sigma_{\text{bar}} = 10^4$, $\omega = 50$, and $\alpha = 10^{-6}$.

Figure 12.2 shows a first, qualitative comparison of the current distribution in a cross section of the plate. Comparing the reference solution[1] with the solution of

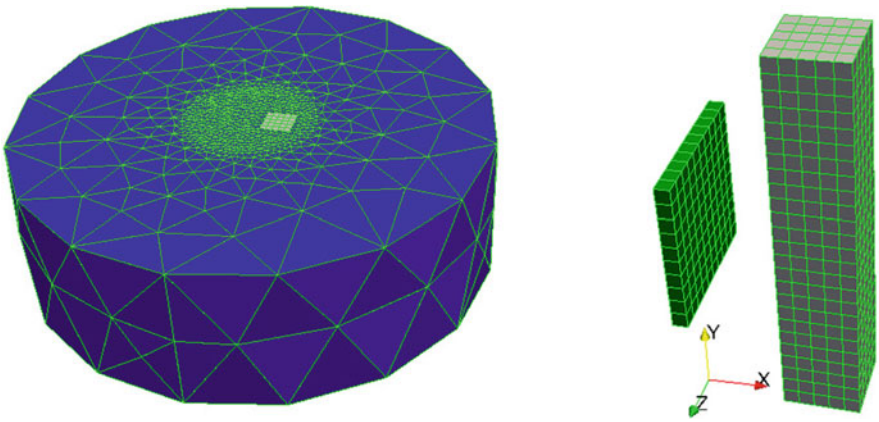

Fig. 12.1 Coarse, hybrid mesh of domain Ω with airbox (left) and without airbox (right), $h = 0.2$

[1]The reference solution was obtained on an refined mesh, which is adapted to the local features of the solution, using second order edge elements.

Fig. 12.2 Current distribution $|\mathbf{j}| = |\omega\sigma\mathbf{A}^\alpha|$ in plate plotted over cross-section $y = 0$ for $\sigma_{\text{plate}} = 5 \cdot 10^7$, $\delta_{\text{plate}}/h = 0.063$

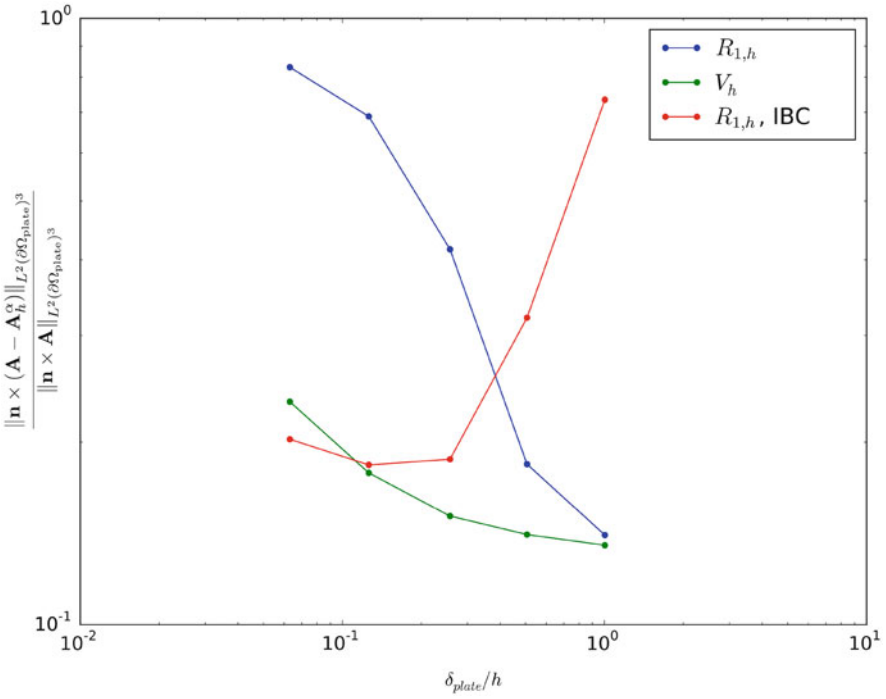

Fig. 12.3 Local surface error vs. skin-depth δ for the mesh shown in Fig. 12.1

the standard, first order FEM, we see that the top and bottom boundary layers are not resolved at all and the behavior in the edges is completely wrong. The proposed (modulated) Trefftz method with $k = 1$ can resolve the bottom and top boundary layer much better but the error is still considerable in the edges.

Figure 12.3 shows the *relative* local surface error $\frac{\|\mathbf{n}\times(\mathbf{A}-\mathbf{A}_h^\alpha)\|_{L^2(\partial\Omega_{\text{plate}})^3}}{\|\mathbf{n}\times\mathbf{A}\|_{L^2(\partial\Omega_{\text{plate}})^3}}$ for different values of σ_{plate} (and hence δ_{plate}). We observe that the error of the enriched

method is always equal or better than simple first-order edge functions $R_{1,h}$. In particular for $\delta \ll h$ the modulated Trefftz functions clearly outperform the classical edge elements, cf. Fig. 12.2. For reference we also show the error for a standard, first-order FEM formulation where the plate has been replaced by IBC [8]. We see that the IBC approximation becomes valid as $\delta_{\text{plate}} \to 0$ and does in fact reach the precision of the enriched method for small δ. The former is expected since for flat surfaces the IBC solution tends to $\mathbf{A}$ with rate $O(\delta^2)$ [6].

12.5 Concluding Remarks

The enriched approximation space V_h can resolve the boundary layers of problem (12.1) *locally* much better than pure, standard first order Nédélec/edge elements. In contrast to IBC, the presented method also resolves the electromagnetic fields inside of the conductor. In particular, it is applicable to cases where the excitation current $\mathbf{j}^i$ generates boundary layers.[2] We remark that the construction of the functions $\mathbf{A}_{F,\boldsymbol{\tau}}$ is based on the same principle that is used to derive the IBC [8]. In particular, both methods perform very well along flat surfaces but lead to considerable error in edges/corners of the geometry where the assumptions of Sect. 12.3 become invalid and the solution shows singular behavior. A more extensive numerical study unveils that the smaller δ, the more the approximation error $\mathbf{A}^\alpha - \mathbf{A}_h^\alpha$ is concentrated in the edges/corners of the plate. I.e. the approximation error is dominated by the error at corners/edges and choosing a higher order of approximation, $k > 1$ in V_h, will generally not improve the approximation. Instead one has to resolve the singularities either by refining the mesh towards edges/corners or by including the singularities in the approximation space V_h. The latter is particularly attractive since this is just another "enrichment" of the approximation space V_h.

However, finding explicit expressions for the singularities of the 3D eddy current problem at corner points is extremely difficult. For the 2D eddy current equation explicit expressions for these singularities exist [4] and can be used to construct a highly efficient method that shows exponential convergence in the polynomial degree k *independent of* δ, that is the method is *robust* in δ in the sense of [9, Definition 3.54]. We will present the details of our investigation of this method in a future work.

Acknowledgements This work has be co-funded by the Swiss Commission for Technology and Innovation (CTI).

[2] This is confirmed by numerical experiments not shown in this work.

References

1. Bachinger, F., Langer, U., Schöberl, J.: Numerical analysis of nonlinear multiharmonic eddy current problems. Technical report, Johannes Kepler University Linz, 2004. SFB-Report No. 2004-01
2. Bergot, M., Duruflé, M.: High-order optimal edge elements for pyramids, prisms and hexahedra. J. Comput. Phys. **232**(1), 189–213 (2013)
3. Casagrande, R.: Discontinuous finite element methods for eddy current simulation. Ph.D. thesis, ETH Zürich (2017)
4. Dauge, M., Dular, P., Krähenbühl, L., Péron, V., Perrussel, R., Poignard, C.: Corner asymptotics of the magnetic potential in the eddy-current model. Math. Methods Appl. Sci. **37**(13), 1924–1955 (2014)
5. Jackson, J.D.: Classical Electrodynamics. Wiley, London (1999)
6. Mitzner, K.: An integral equation approach to scattering from a body of finite conductivity. Radio Sci. **2**(12), 1459–1470 (1967)
7. Monk, P.: Finite Element Methods for Maxwell's Equations. Oxford University Press, Oxford (2003)
8. Ostrowski, J.: Boundary element methods for inductive hardening. Ph.D. thesis, Universität Tübingen (2002)
9. Schwab, C.: p-and hp-Finite Element Methods: Theory and Applications in Solid and Fluid Mechanics. Oxford University Press, Oxford (1998)
10. Xenophontos, C.: The hp finite element method for singularly perturbed problems in nonsmooth domains. Numer. Methods Partial Differ. Equ. **15**(1), 63–90 (1999)